

Characterization by Thermal Analysis of High Density Polyethylene/Polypropylene Blends with Enhanced Biodegradability

L. Contat-Rodrigo,¹ A. Ribes-Greus,¹ C. T. Imrie²

¹ *Departamento Termodinamica Aplicada, ETSII Universidad Politecnica de Valencia, P. O. Box 22012, E-46071, Spain*

² *Department of Chemistry, University of Aberdeen, Neston Walk, Old Aberdeen, AB24 3UE, United Kingdom*

Received 16 May 2001; accepted 14 January 2002

ABSTRACT: Blends of high density polyethylene (HDPE) and polypropylene (PP) with different biodegradable additives have been subjected to an outdoor soil burial test. The effect of the degradation process on the structural and morphological properties of the samples has been studied by thermogravimetry, differential scanning calorimetry, and dynamic-mechanical spectroscopy. The thermogravimetric results show that the additive is more affected by the degradation process than the polymeric matrix. Changes both

in the crystalline morphology and the activation energies of the relaxation processes take place in different stages, and can be described using polynomial equations. These changes occur on different time scales depending on the additive used. © 2002 Wiley Periodicals, Inc. *J Appl Polym Sci* 86: 174–185, 2002

Key words: polyolefins; blends; thermogravimetric analysis; differential scanning calorimetry; viscoelastic properties

INTRODUCTION

Polyolefins constitute one of the most important classes of plastics both in their widespread use and production volume, and are considered to be inert polymers. This is so because microorganisms are unable to metabolize them in acceptable periods of time.¹ This inert character is due, largely, to their hydrophobic nature and their large molecular size. However, it is possible to obtain polyolefins with enhanced biodegradability through the incorporation of additives containing, among others, readily biodegradable natural polymers, such as starch. The degradation of these additives leaves a weakened polymeric matrix, which is more susceptible to undergo biodegradation.

This idea was introduced by Griffin in the 1970s.² Since then, formulations of biodegradable additives have been ascribed to him, which consist mainly of granular starch, a prooxidant and low density polyethylene in the form of a masterbatch. Polyolefins filled with these products can be degraded as the result of the synergetic action of biotic and abiotic degradation mechanisms.^{3–7} Later, other type of materials has also been developed, consisting of starch in its destructuralized form and synthetic polymers.^{8,9}

One possible application of such polyolefins with enhanced biodegradability is in the manufacture of

pots and seedboxes. These would allow plants to grow adequately in seedbeds, and subsequently, biodegrade in the soil in which they are buried. In this way, the plants do not need to be transplanted, and thus the risk of damage to the plants is avoided. The objective of this work is to study, using thermal analysis, the biodegradation process of HDPE/PP blends filled with differing biodegradable additives when subjected to an outdoor soil burial test.

EXPERIMENTAL

Materials

High density polyethylene 5218 (HDPE) supplied by British Petroleum (Spain) and polypropylene 1148-TC (PP) from BASF (Germany) were used as the polymeric matrix.

A 92/8% (by weight) rice granular starch and iron oxide mixture, Bioeffect 72000 (Proquimaq Color, S.L., Spain) and Mater-Bi AF05H (Novamont, U.S.A.) were used as the biodegradable additives. Bioeffect combines 75% low density polyethylene (LDPE), 20% starch, and 5% prooxidants containing fatty acids. Mater-Bi AF05H contains thermoplastic starch heavily complexed with ethylene-vinyl alcohol (EVOH) copolymers.

Samples

Three types of samples labeled A, B, and C have been prepared. Each consist of a 40/60% (by weight)

Correspondence to: A. R. Greus (aribes@ter.upv.es).

TABLE I
Biodegradable Additives Used in Each Sample

Sample	Additive
A	Rice starch/iron oxide (92/8% by weight)
B	Bioeffect 72000
C	Mater-Bi AF05H

HDPE/PP blend with 10% (by weight) of a biodegradable additive. Sample A contains the rice starch/iron oxide mixture as the additive, sample B includes Bioeffect, and sample C contains Mater-Bi (Table I). All the samples have been processed by injection as seed-boxes.

Soil burial test

The samples have been subjected to an outdoor soil burial test in Ayora (Valencia, Spain) for 21 months. They have been buried in soil normally used for the growth of pines, and this has a pH of 6.75 (measured in water). Monthly average temperatures in Ayora during the soil burial test are given in Table II.

Samples were removed after differing periods of time: 0, 3, 6, 9, 12, 15, and 21 months. After removal, each sample was carefully washed using a soap solution in order to stop the biodegradation process, and dried with a piece of paper prior to analysis.

Thermogravimetric analysis

The thermogravimetric analysis of the samples was carried out using a Mettler-Toledo thermogravimetric analysis/single differential thermal analysis (TGA/

TABLE II
Monthly Average Temperature in Ayora (Valencia, Spain) During the Soil Burial Test

Month	T (°C)		
	1996	1997	1998
January	10.2	8.4	9.0
February	8.0	11.0	10.2
March	10.9	12.4	13.2
April	14.4	15.2	13.8
May	17.4	18.0	16.2
June	22.2	21.6	23.0
July	25.3	23.2	26.7
August	25.1	24.8	26.0
September	19.6	22.0	22.6
October	16.5	18.4	16.3
November	12.2	12.8	11.7
December	9.0	9.4	6.6

SDTA) 851 module. Dynamic measurements were performed from 25 to 600°C at a heating rate of 10°C/min under argon atmosphere (flow rate = 200 mL/min). The samples' masses were about 10 mg. The thermodegradation products were analyzed using a coupled Balzers ThermoStar mass spectrometer. Molecular weights between 0 and 200 amu were determined.

Differential scanning calorimetry

The morphology of the samples was studied by differential scanning calorimetry (DSC) using a Perkin Elmer DSC-4 calorimeter, previously calibrated with indium. Five to six milligrams of sample was weighed out in a standard aluminum pan. The sealed pans were scanned at a heating rate of 10°C/min from 0 to

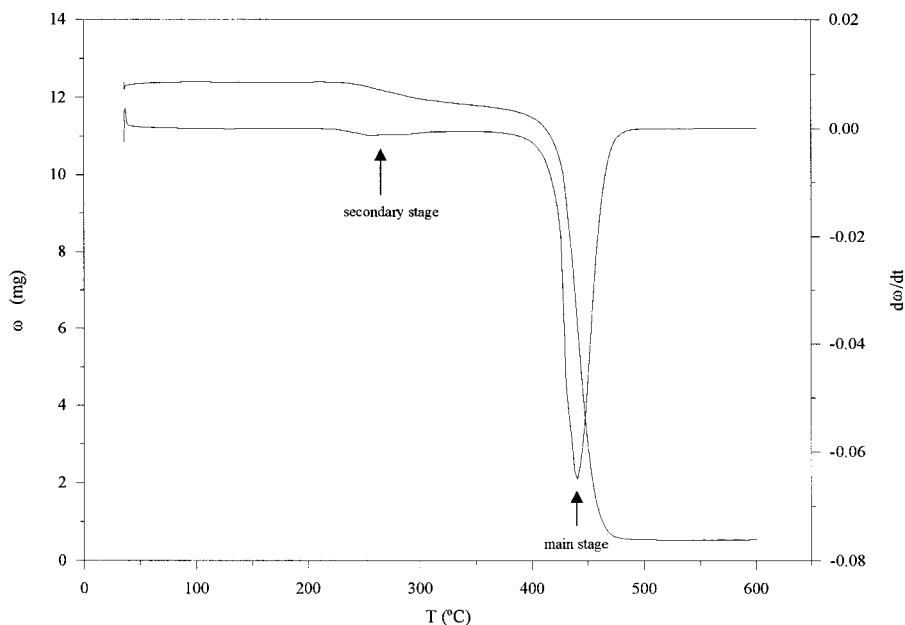


Figure 1 TG and DTG thermograms of the undergraded sample A.

TABLE III
Thermogravimetric Results of Sample A as a Function of the Exposure Time in Soil

Exposure time (months)	Total mass loss (%)	Residue (%)	Mass loss secondary stage (%)	Mass loss main stage (%)	Peak temp. secondary stage (°C)	Peak temp. main stage (°C)
0	90.4	9.6	2.4	88.2	254.2	440.6
12	95.4	4.6	2.4	87.8	233.7	446.1
21	95.7	4.3	1.8	87.7	275.5	445.5

200°C under a nitrogen atmosphere. Measurements were repeated until errors of less than ± 0.05 for crystalline contents were assured.

Dynamic mechanical measurements

Viscoelastic properties were determined by means of a Polymer Laboratories Dynamic Mechanical Thermal Analyzer, MARK II DMTA. Deformation was applied in the cantilever double-clamping flexure mode. The storage modulus, E' , and the loss tangent, $\tan \delta$, were measured from -140 to 160°C at frequencies of 0.3, 1, 3, 10, and 30 Hz with a heating rate of $1^\circ\text{C}/\text{min}$.

RESULTS AND DISCUSSION

Thermogravimetry

The undegraded samples and those degraded in soil for 12 and 21 months have been characterized by thermogravimetry. All the samples exhibit basically the same thermograms regardless of the additive used and the exposure time. Specifically, two well-defined stages can be observed in the TG and differential thermogravimetric (DTG) thermograms of all the samples (Fig. 1). A secondary thermodegradation process occurs between ca. 250 and 300°C during which only 2–4% of the sample mass is lost. The main weight loss occurs at about 450°C . This stage has been assigned to the complete degradation of the carbon chains of the polymeric matrix, which constitute the main component of the samples. Tables III, IV, and V show the thermogravimetric results of samples A, B and C respectively. It is observed that, in general, the residue tends to decrease as the exposure time in soil increases, regardless of the additive used. This tendency is regular for samples A and C, but not for sample B,

for which the residue initially increases before starting to decrease.

The temperature of the main stage of degradation does not change significantly with the exposure time in soil. This indicates that the polymeric matrix is not modified to any great extent during the degradation process in soil.

On the other hand, the temperature of the secondary thermodegradation process increases initially and decreases after longer exposure for samples B and C, while for sample A it exhibits the opposite trend. Furthermore, this temperature differs depending on the additive used. These values,² together with the differences observed in this secondary stage between the three types of samples, strongly suggest that this process can be attributed to the thermal degradation of the additive, as this is the only component that is different from one sample to another.

In order to analyze in more detail these thermogravimetric results, the kinetics of each reaction has been studied by means of the Hirata differential method.¹⁰ Hirata describes the kinetics of a system undergoing chemical changes in terms of the weight of the sample at time t , ω :

$$\frac{d\omega}{dt} = -k(T) \cdot \omega \quad (1)$$

where k is the rate constant of the reaction, which is dependent on temperature. This dependence is generally expressed by means of the Arrhenius equation:

$$k(T) = A \exp\left(\frac{-E}{RT}\right) \quad (2)$$

where R is the gas constant, T is the absolute temperature, E is the activation energy, and A is the preexponential factor.

TABLE IV
Thermogravimetric Results of Sample B as a Function of the Exposure Time in Soil

Exposure time (months)	Total mass loss (%)	Residue (%)	Mass loss secondary stage (%)	Mass loss main stage (%)	Peak temp. secondary stage (°C)	Peak temp. main stage (°C)
0	97.0	3.0	2.1	93.6	286.8	448.4
12	95.2	4.8	1.4	91.2	301.0	449.3
21	96.7	3.3	2.3	91.8	294.8	450.0

TABLE V
Thermogravimetric Results of Sample C as a Function of the Exposure Time in Soil

Exposure time (months)	Total mass loss (%)	Residue (%)	Mass loss secondary stage (%)	Mass loss main stage (%)	Peak temp. secondary stage (°C)	Peak temp. main stage (°C)
0	94.3	5.7	3.9	79.2	297.0	454.5
12	94.8	5.2	2.7	81.6	306.3	454.5
21	95.7	4.8	1.1	83.3	304.8	453.3

Substituting the Arrhenius equation into eq. (1) and taking logarithms, yields the Hirata equation:

$$\ln\left(-\frac{d\omega}{dt}\right) - \ln\omega = \ln A - \frac{E}{RT} \quad (3)$$

Thus, a plot of $[\ln(-d\omega/dt) - \ln\omega]$ vs the reciprocal of temperature should give a straight line for each process, from which the activation energy and the preexponential factor can be calculated.

Table VI summarizes the activation energies calculated with the Hirata method for sample A. It has been found that the thermodegradation of this sample takes place in two stages. As stated previously, the main stage (407–444°C) corresponds to the thermal decomposition of the carbon backbones. However, by means of the Hirata method it is not possible to distinguish this from the thermodegradation of HDPE and PP. The activation energy slightly decreases with the exposure time in soil, suggesting a certain breakdown of the carbon chains as a consequence of the biodegradation process.

The secondary degradation stage (233–253 and 256–268°C) appears as a complex process that occurs in the degradation regime of starch.² In general, it can be observed that the activation energy decreases with the exposure time. This indicates the degradation of the additive in sample A.

The values of the activation energies determined for sample B are shown in Table VII. The thermodegradation of this sample is a complex process. The nature and the origin of each of the processes involved in this thermal degradation cannot be assigned unambiguously. This is the case because sample B contains HDPE, PP, starch, and LDPE as a component of Biofect.

The activation energies of the stages taking place at higher temperatures (372–407 and 407–444°C) do not vary with the exposure time in soil. Due to the temperature range over which these processes occur, they can be attributed to the thermodegradation of the carbon backbones. Thus, the results indicate that biodegradation scarcely affects the chemical structures of the polymeric matrix in sample B.

The most sensitive process to the exposure time in soil is that taking place between 262 and 283°C. This process has been assigned by other authors to the thermodegradation of starch,² although the values of the activation energy reported here are too high to suppose that they are exclusively due to the starch. From the analysis of the variation of the activation energy with the exposure time, it is observed that this parameter does not decrease uniformly, suggesting that this stage is in fact a complex process in which not only starch is involved. This could explain the excessively high values found for the activation energy of this stage.

Table VIII summarizes the results obtained for sample C. These show that the thermodegradation of sample C also takes place in two stages. As previously stated, the main stage (407–457°C) corresponds to the degradation of the carbon backbones. That the activation energy of this process does not change with the exposure time suggests that the polymeric matrix of sample C has also not been affected by biodegradation. The secondary stage (192–256 and 256–298°C) is a complex process that appears in the thermodegradation regime of starch.² In general, it is observed that the activation energy decreases, thus indicating the biodegradation of the Mater-Bi additive.

The principle volatile products produced during the thermal degradation of the samples under study are

TABLE VI
Apparent Activation Energies, E_a , of Sample A Calculated with the Hirata Method as a Function of the Exposure Time in Soil

Exposure time (months)	T (°C)	E_a (kcal/mol)	T (°C)	E_a (kcal/mol)	T (°C)	E_a (kcal/mol)
0	407–444	103.4	256–268	—	233–253	27.9
12	407–444	90.1	256–268	8.8	233–253	—
21	407–444	92.2	256–268	11.5	233–253	—

TABLE VII
Apparent Activation Energies, E_a , of Sample B Calculated with the Hirata Method
as a Function of the Exposure Time in Soil

Exposure time (months)	T (°C)	E_a (kcal/mol)	T (°C)	E_a (kcal/mol)	T (°C)	E_a (kcal/mol)
0	407–444	80.3	372–407	54.2	262–283	73.2
12	407–444	77.3	372–407	52.4	262–283	55.4
21	407–444	78.7	372–407	52.2	262–283	64.6

listed in Table IX. The mass spectrometry analysis reveals that the thermodegradation of samples A, B and C is essentially complete, since only products with low molecular weights have been detected. Larger fragments emanating from the carbon backbones have not been obtained. This suggests that during the thermodegradation process, transfer reactions have not been favoured in samples subjected to the outdoor soil burial test.^{11,12}

DSC

The morphological changes undergone by samples A–C during degradation in soil have been probed by DSC. Figure 2 shows the DSC thermograms of sample B as a function of the exposure time in soil. Similar curves have been obtained for samples A and C.

The thermograms of all the samples clearly contain endotherms at ca. 129°C, associated with the melting of HDPE, and at ca. 166°C associated with the melting of PP. These results prove the heterogeneous nature of the HDPE/PP blend used as the polymeric matrix.^{13,14}

The total crystalline contents of HDPE and PP in the samples have been calculated according to the following equation:

$$X = \frac{(H_a - H_c)}{H_m} \quad (4)$$

where H_a and H_c are the enthalpies in the melt state and the crystalline state, respectively. Their difference is directly obtained from the thermogram. H_m is the change in the melting enthalpy of a perfect crystal of

infinite size; for PE, $H_m = 70$ cal/g and for PP, $H_m = 50$ cal/g.¹⁴

The change in the crystalline contents of HDPE and PP with the exposure time in soil has been studied (Figs. 3–5). In general, no uniform variation of crystallinity has been found, but changes have been found to be more significant for PP.

This result is in agreement with the well-known fact that PP is more susceptible to oxidation than polyethylene due to its methyl branches all along the backbone.^{11,15} At the branch points, there is a hydrogen attached to a tertiary carbon, which is more labile than the hydrogens of the methyl groups of the backbone chain. Thus, these labile hydrogens are more likely sites for the initiation of the oxidation process. According to the biodegradation mechanism of polyolefins proposed by Albertsson,¹⁶ a previous abiotic oxidation is necessary, so that carbonyl groups are formed and the biodegradation process could then be later performed by microorganisms. Thus, the more oxidable is a polymeric matrix (such as polypropylene in this case), the more susceptible to undergo biodegradation it will be.

On the other hand, it has also been observed that the crystalline content successively increases and decreases with the exposure time and these changes can be adequately fitted to polynomial equations. Similar behaviour has also been obtained by other authors when studying degradation effects on the properties of polyolefins in terms of parameters such as the elongation at break.^{17,18}

This behavior agrees with the proposal of Albertsson et al.¹⁹ that degradation leads to changes in the

TABLE VIII
Apparent Activation Energies, E_a , of Sample C Calculated with the Hirata Method
as a Function of the Exposure Time in Soil

Exposure time (months)	T (°C)	E_a (kcal/mol)	T (°C)	E_a (kcal/mol)	T (°C)	E_a (kcal/mol)
0	407–457	79.0	256–298	21.1	192–256	14.3
12	407–457	80.5	256–298	19.6	192–256	14.0
21	407–457	79.9	192–298	16.4	192–256	–

TABLE IX
Principle Decomposition Products Detected
by Mass Spectroscopy

Amu	Corresponding chemical structures
14	CH ₂
15	CH ₃
16	CH ₄
18	H ₂ O
28	CO, C ₂ H ₄
30	C ₂ H ₆
32	O ₂
44	C ₂ H ₄ O, CO ₂

crystalline morphology of polyolefins that take place in different stages. On the other hand, Hawkins has suggested that a scission of the chains in the amorphous regions caused by oxidation, gives rise to a higher degree of crystallinity.¹⁵ Thus, such an increase in crystallinity could be then considered as a measure of degradation.

In this case, samples A and C exhibit more significant changes in their HDPE and PP crystalline contents than sample B. Therefore this suggests that these

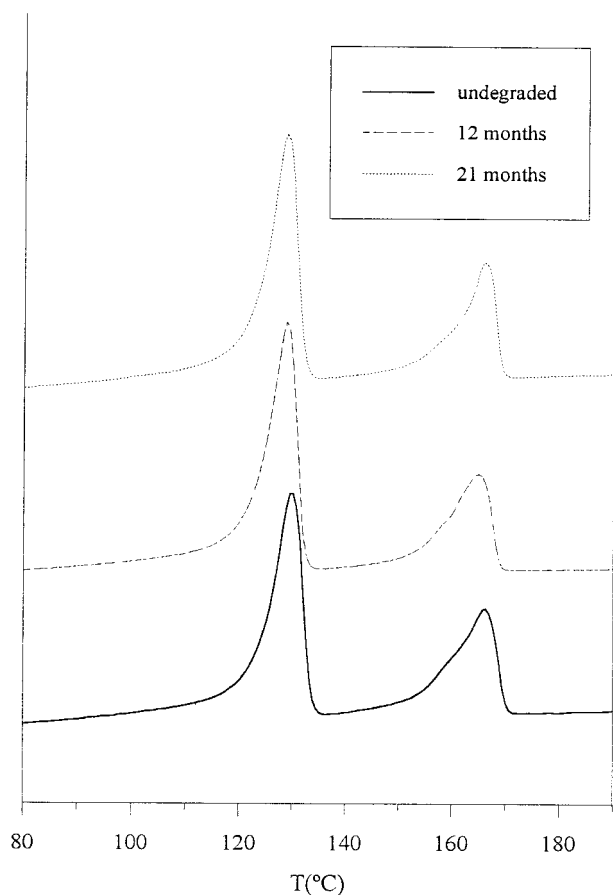


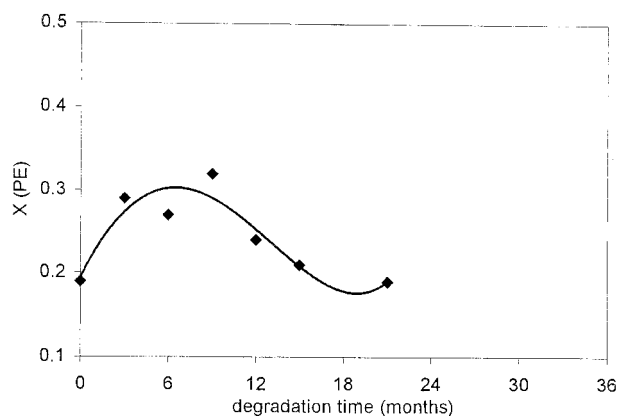
Figure 2 DSC thermograms of sample B after different exposure times.

samples have been more affected by the degradation process.

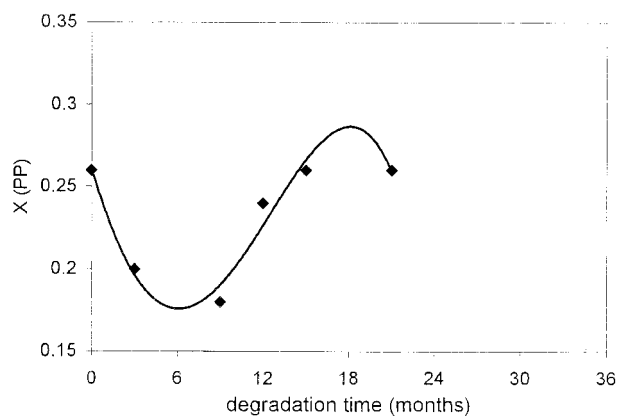
DMTA

The viscoelastic properties of the polymers have also been studied as a function of the exposure time in soil. For this purpose, the complete relaxation spectra of all the samples have been obtained. Figure 6 shows, for example, the mechanical relaxation spectrum of sample B in terms of the storage modulus (E') and the loss tangent ($\tan \delta$) for different exposures times. Similar spectra have been obtained for samples A and C.

It has been found that the degradation process modifies the storage modulus. Initially E' increases with the exposure time but subsequently decreases. Furthermore, it is observed that the storage modulus of the

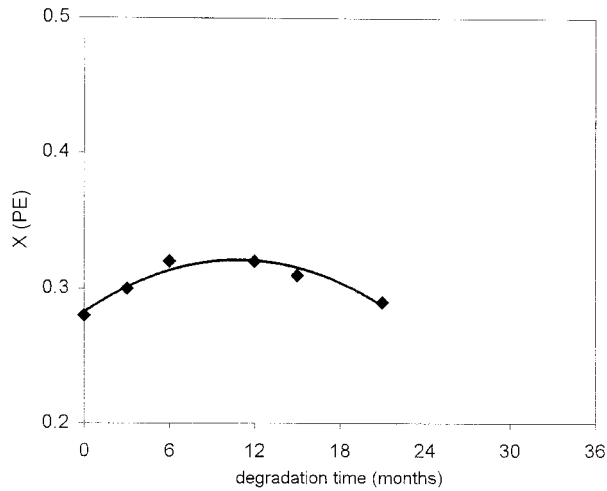


(a)

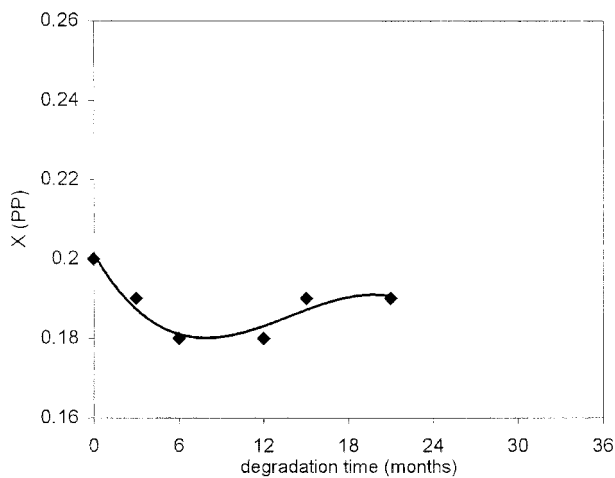


(b)

Figure 3 Evolution with the exposure time in soil of the crystalline content, X , of (a) HDPE and (b) PP in sample A. Polynomial fit for (a): $y = [2 \cdot 10^{-6} \cdot x^4] + [3 \cdot 10^{-5} \cdot x^3] - (0.0032 \cdot x^2) + (0.036 \cdot x) + 0.1935$ ($r^2 = 0.8481$). Polynomial fit for (b): $y = [2 \cdot 10^{-6} \cdot x^4] - [9 \cdot 10^{-6} \cdot x^3] + (0.0027 \cdot x^2) - (0.0294 \cdot x) + 0.2612$ ($r^2 = 0.9445$).



(a)



(b)

Figure 4 Evolution with the exposure time in soil of the crystalline content, X , of (a) HDPE and (b) PP in sample B. Polynomial fit for (a): $y = (-0.0003 \cdot x^2) + (0.0071 \cdot x) + 0.2823$ ($r^2 = 0.934$). Polynomial fit for (b): $y = [-10^{-5} \cdot x^3] + (0.0005 \cdot x^2) - (0.0062 \cdot x) + 0.2012$ ($r^2 = 0.901$).

degraded samples during the soil burial test is always higher than that of the corresponding undegraded sample.

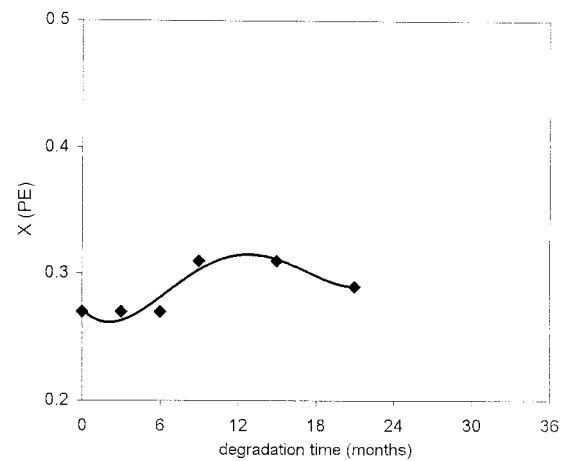
In the spectra plotted in terms of the loss tangent, the three relaxation zones, denoted α , β , and γ in order of decreasing temperature, can be clearly distinguished (Fig. 6). These results are in good agreement with the relaxation spectra predicted in the literature for HDPE/PP blends,²⁰ Boyd,²¹ Popli,²² and ourselves²³ have established that the α relaxation can be attributed to movements of molecular chains that oc-

cur in crystalline regions. The β relaxation may result from motions taking place at the crystalline–amorphous interface. The γ relaxation can be associated to molecular chain movements in the amorphous phase of polyethylene.

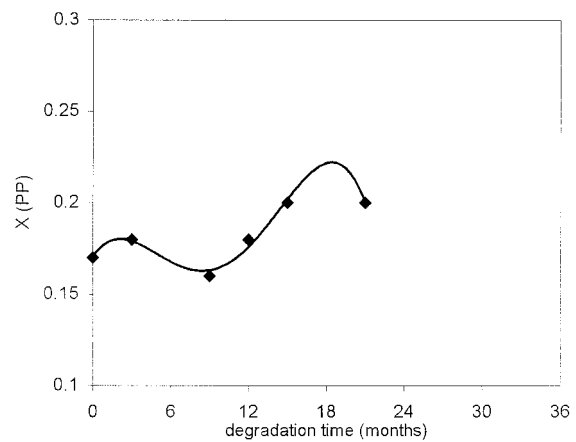
The apparent activation energy, E_a , of each relaxation has been calculated (with an accuracy of ± 1 kcal/mol) by fitting the dependence of the mean relaxation times on the temperature to the Arrheni

$$\ln f_m = \ln f_0 + \exp(E_a/RT) \quad (5)$$

where T_m and f_m are the temperature and the frequency of the maximum of the loss modulus, respec-



(a)



(b)

Figure 5 Evolution with the exposure time in soil of the crystalline content, X , of (a) HDPE and (b) PP in sample C. Polynomial fit for (a): $y = [5 \cdot 10^{-6} \cdot x^4] - [3 \cdot 10^{-4} \cdot x^3] + (0.0033 \cdot x^2) - (0.0107 \cdot x) + 0.2716$ ($r^2 = 0.8821$). Polynomial fit for (b): $y = [-8 \cdot 10^{-6} \cdot x^4] + [3 \cdot 10^{-4} \cdot x^3] - (0.0033 \cdot x^2) + (0.0104 \cdot x) + 0.1704$ ($r^2 = 0.9757$).

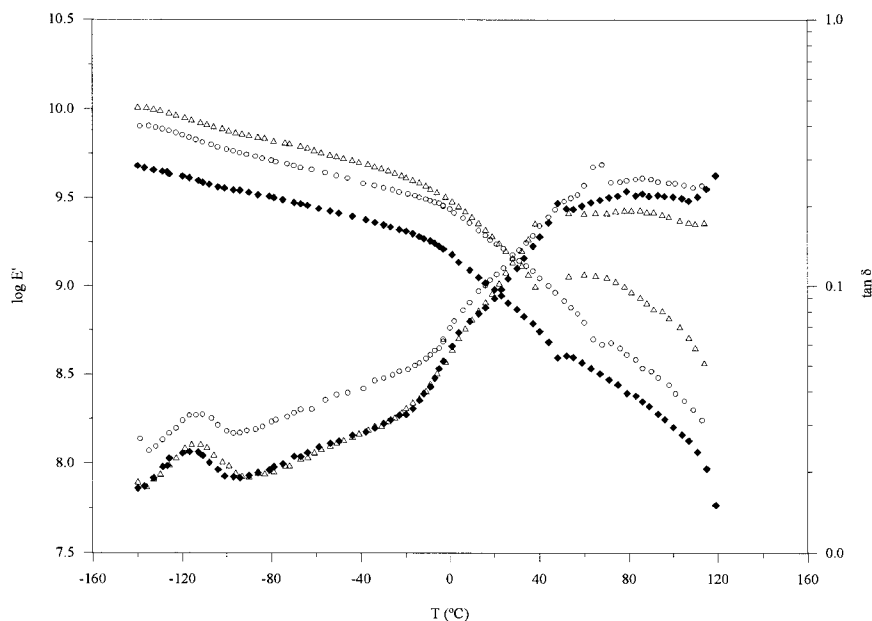


Figure 6 Log E' and $\tan \delta$ vs temperature for sample B at 1 Hz of frequency for different exposure times: \blacklozenge , undergraded; \triangle , 12 months; \circ , 21 months.

tively. T_m has been determined by means of the Fuoss–Kirkwood equation:

$$E'' = \frac{E''_{max}}{\cosh m \frac{E_a}{R} \left(\frac{1}{T} - \frac{1}{T_m} \right)} \quad (6)$$

where E''_{max} is the maximum of the loss modulus and m is the Fuoss–Kirkwood parameter.

In Figure 7, the activation energy of the γ relaxation is plotted against the degradation time in soil for samples A, B, and C respectively. It can be seen that the activation energy of this relaxation changes in different stages with the exposure time, as do other morphological and structural parameters. These changes can also be adequately represented by polynomial equations. All the samples display a minimum activation energy, which appears after 12 months of exposure for samples A and B, and around 8 months for sample C. On the other hand, the γ relaxation of sample C exhibits the lowest activation energy at the end of the soil burial test. Within the framework that the γ relaxation is related to motions of the molecular chains that form the amorphous phase, these results indicate that the amorphous regions of sample C are more readily affected by degradation than those in samples A and B.

The β relaxation zone of the samples under study is very complex, since it results from overlapping relaxations of HDPE, PP, and the corresponding additive.²⁴ Moreover, it appears as a weak relaxation, of low

intensity (Fig. 6). As a consequence, the characterization of the β relaxation zone of these samples is a difficult task. It has only been possible to calculate the activation energy of the β relaxation of sample C after 15 and 21 months' exposure, at which stage the β relaxation becomes more prominent (Fig. 8). Activation energies of 63 and 70 kcal/mol have been obtained for sample C degraded for 15 and 21 months, respectively. Similar activation energies have been found for the β_{II} relaxation of pure Mater-Bi (65 kcal/mol)²⁴ and for the β relaxation of samples similar to sample C, but whose polymeric matrix is only made up of PP (66–43 kcal/mol depending on the exposure time).²⁴

It has been found by these authors that Mater-Bi exhibits great biodegradability in soil.²⁴ The removal of the additive as a consequence of its biodegradation could lead to a less constrained polymeric matrix. This would facilitate the movements of the backbones of HDPE and PP, allowing a more prominent β relaxation to be observed. The β relaxation of the undergraded Mater-Bi that may still remain, could also contribute to this complex peak.

By contrast, the α relaxation displays a great intensity in the spectra of all the samples (Figs. 6 and 8). This relaxation has been decomposed into two subrelaxations, called α_I and α_{II} in order of increasing temperature. The deconvolution of the relaxations has been carried out with the deconvolution method proposed by Charlesworth,²⁶ together with the Fuoss–Kirkwood equation. This method considers the exper-

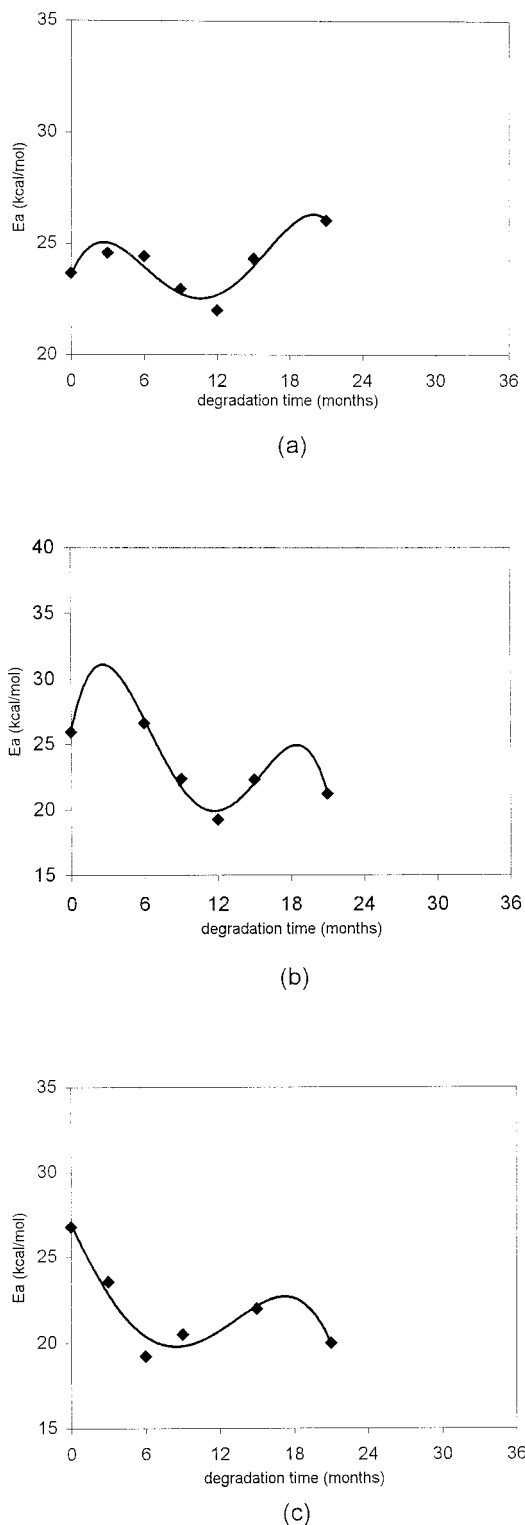


Figure 7 Evolution with the exposure time in soil of the activation energy of the γ relaxation of (a) sample A, (b) sample B, and (c) sample C. Polynomial fit for (a): $y = [-6 \cdot 10^{-4} \cdot x^4] + (0.0249 \cdot x^3) - (0.33 \cdot x^2) + (1.2752 \cdot x) + 23.546$ ($r^2 = 0.8931$). Polynomial fit for (b): $y = [-2 \cdot 10^{-3} \cdot x^4] + (0.0862 \cdot x^3) - (1.1665 \cdot x^2) + (4.4848 \cdot x) + 25.902$ ($r^2 = 0.9765$). Polynomial fit for (c): $y = [-3 \cdot 10^{-4} \cdot x^4] + (0.0064 \cdot x^3) + (0.0539 \cdot x^2) - (1.5843 \cdot x) + 26.943$ ($r^2 = 0.9391$).

perimental data of the loss modulus as the sum of each of the contributions:

$$E'' = \sum_{i=1}^n E''_i \quad (7)$$

Figure 9 gives as example the deconvolution of the α relaxation zone of the undegraded sample A. The activation energies of both α relaxations have also been determined.

Figure 10 shows the change with exposure time of the activation energy of the α_1 relaxation for samples A–C. It has been found that the activation energy increases and decreases successively for all the samples. However, different time scales are observed depending on the additive used. In general, the activation energy of sample B changes most slowly. This indicates that this sample is more resistant to biodegradation than samples A and C.

On the other hand, the high values obtained for the apparent activation energy of the α_1 relaxation suggest that this relaxation can be associated to cooperative movements of the molecular chains that form the amorphous and interfacial regions, similar to the glass transition of amorphous polymers. In this sense, such movements could trigger motions in the crystalline phase itself, which will result in the α_{II} relaxation.

Figure 11 shows the evolution with the exposure time of the activation energy of the α_{II} relaxation for all the samples. As it has been already in the case of the γ and α_1 relaxations, the evolution curve follows a polynomial tendency with the exposure time in soil.

Also as with the α_1 relaxation, the apparent activation energy of the α_{II} relaxation changes on different time scales depending on the additive used. While samples A and B undergo changes on similar time scales, changes in sample C occur at shorter times. For this sample, the first maximum of E_a is not observed and the second one appears before that for samples A and B. This indicates that the crystalline phase of sample C is faster affected by the degradation process.

CONCLUSIONS

The thermogravimetric analysis shows two thermo-degradation processes for all the samples. The main stage has been attributed to the complete decomposition of the carbon backbones of HDPE and PP. The secondary stage has been assigned to the thermal degradation of the corresponding additive. In general, the thermogravimetric results have proved the additive to be more affected by the degradation process in soil than the polymeric matrix.

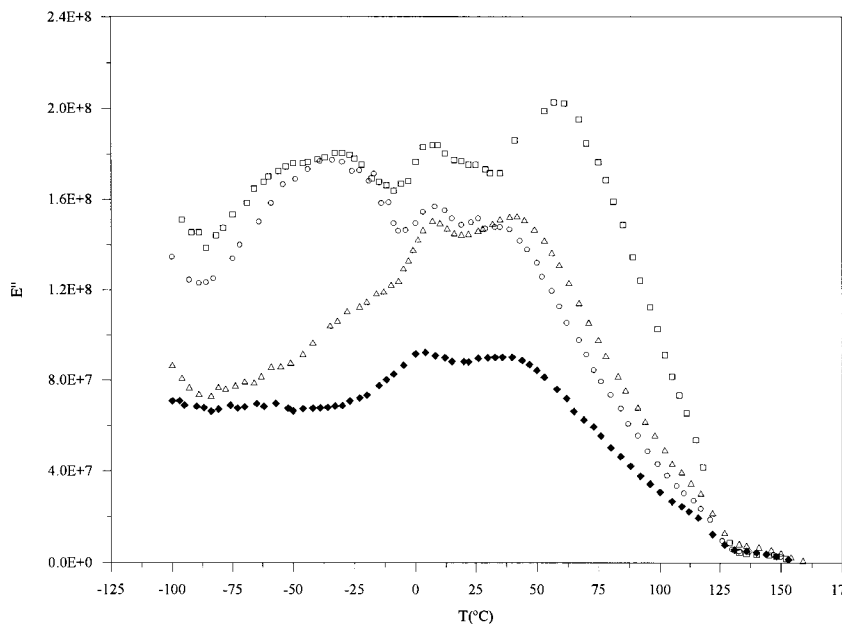


Figure 8 E'' vs temperature for sample C at 1 Hz of frequency for different exposure times: \blacklozenge , undegraded; \triangle , 3 months; \circ , 12 months; \square , 21 months.

Changes in the crystalline morphology of both HDPE and PP during degradation in soil occur in different stages. Such evolution can be adequately represented by polynomial equations. Changes have been found to be more significant for PP.

As for these morphological parameters, the evolution with the exposure time of the apparent activation energy of the γ , α_I , and α_{II} relaxations also takes place in different stages. The complexity and the low intensity of the β relaxation in most of the samples have hindered an accurate characterization of this relaxation.

Sample B is the most resistant to the degradation process. Degradation in soil scarcely affects the chemical structures of its polymeric matrix and it undergoes morphological changes more slowly.

Sample C is the one displaying more significant morphological changes during degradation in soil. This sample exhibits changes in its crystallinity and the activation energies of its relaxations at shorter times than the other samples.

Sample A is the one showing more significant structural changes with the exposure time. A certain deg-

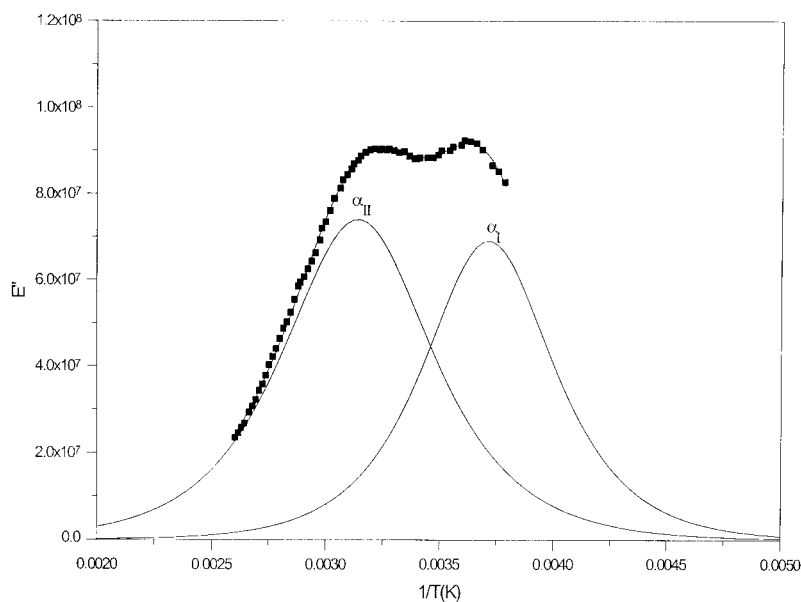
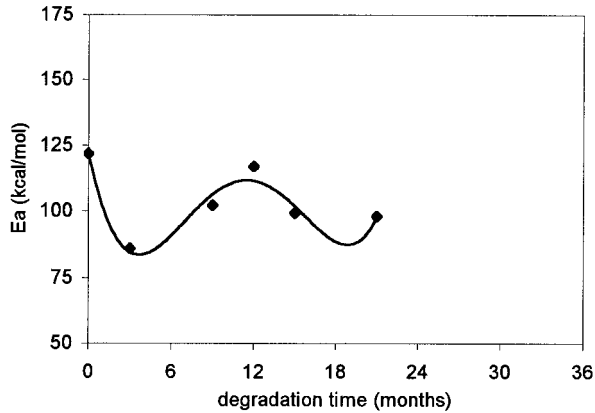
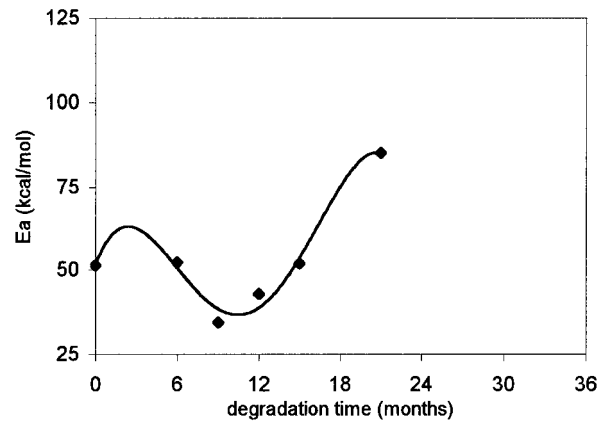


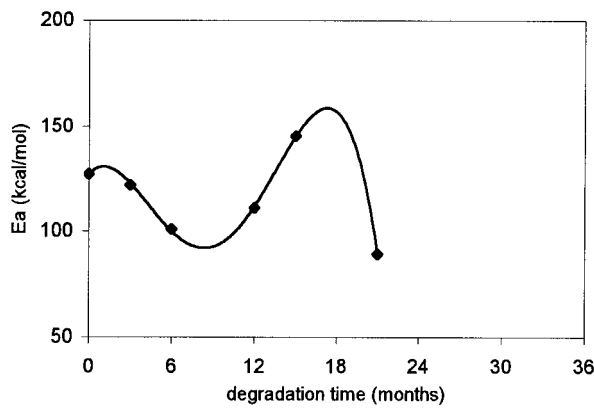
Figure 9 Deconvolution in terms of E'' of the α relaxation of the undegraded sample A at 1 Hz of frequency.



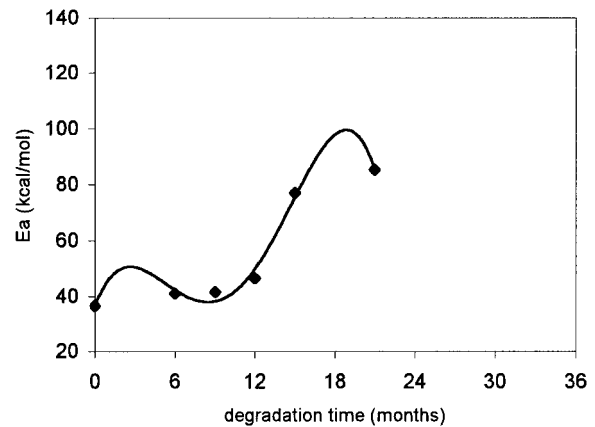
(a)



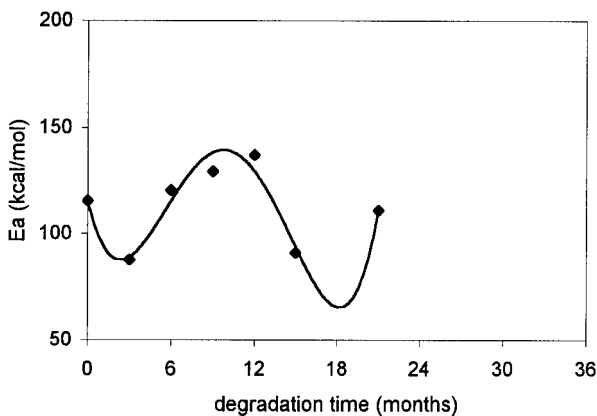
(a)



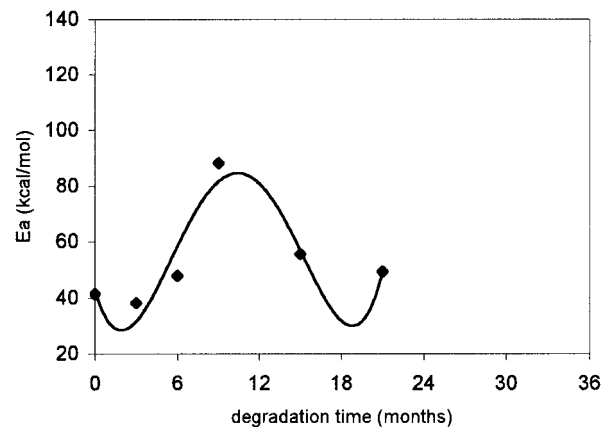
(b)



(b)



(c)



(c)

Figure 10 Evolution with the exposure time in soil of the activation energy of the α_I relaxation of (a) sample A, (b) sample B, and (c) sample C. Polynomial fit for (a): $y = (0.0079 \cdot x^4) - (0.3568 \cdot x^3) + (5.1625 \cdot x^2) - (25.068 \cdot x) + 122.3$ ($r^2 = 0.9341$). Polynomial fit for (b): $y = (-0.0119 \cdot x^4) + (0.4237 \cdot x^3) - (4.0921 \cdot x^2) + (7.3729 \cdot x) + 126.91$ ($r^2 = 0.9988$). Polynomial fit for (c): $y = (0.016 \cdot x^4) - (0.6456 \cdot x^3) + (7.7904 \cdot x^2) - (26.938 \cdot x) + 115.74$ ($r^2 = 0.918$).

Figure 11 Evolution with the exposure time in soil of the activation energy of the α_{II} relaxation of (a) sample A, (b) sample B, and (c) sample C. Polynomial fit for (a): $y = (-0.0052 \cdot x^4) + (0.2342 \cdot x^3) - (3.0457 \cdot x^2) + (10.828 \cdot x) + 51.475$ ($r^2 = 0.9744$). Polynomial fit for (b): $y = (-0.0075 \cdot x^4) + (0.2979 \cdot x^3) - (3.4596 \cdot x^2) + (12.628 \cdot x) + 36.433$ ($r^2 = 0.9876$). Polynomial fit for (c): $y = (0.0109 \cdot x^4) - (0.4529 \cdot x^3) + (5.4997 \cdot x^2) - (16.466 \cdot x) + 42.887$ ($r^2 = 0.8777$).

radiation of its polymeric matrix is manifested by a slight decrease in the activation energy of its thermo-degradation.

REFERENCES

1. Ohtake, Y.; Kobayashi, T.; Asabe, H.; Murakami, N.; Ono, K. *J Appl Polym Sci* 1998, 70, 1643.
2. Griffin, G. J. L., Ed. *Chemistry and Technology of Biodegradable Polymers*; Blackie Academic & Professional: Glasgow, 1994.
3. Hakkarainen, M.; Albertsson, A.-C.; Karlsson, S. *J Appl Polym Sci* 1997, 66, 959.
4. Sastry, P. K.; Satyanarayana, D.; Mohan Rao, D. V. *J Appl Polym Sci* 1998, 70, 2251.
5. Erlandsson, B.; Karlsson, S.; Albertsson, A.-C. *Polym Degrad Stab* 1997, 55, 237.
6. Johnson, K. E.; Pometto, A. L., III; Nikolov, Z. L. *Appl Environ Microbiol* 1993, 59(4), 1155.
7. Greizerstein, H. B.; Syracuse, J. A.; Kostyniak, P. J. *Polym Degrad Stab* 1993, 39, 251.
8. Bastioli, C. *Polym Degrad Stabil* 1998, 59, 263.
9. Bastioli, C.; Degli Innocenti, F.; Guanella, I.; Romano, G. In *Degradable Polymers, Recycling and Plastic Waste Management*; Albertsson, A. C., Huang, S. J., Eds.; Marcel Dekker: New York, 1995; p 247.
10. Hirata, T.; Werner, K. E. *J Appl Polym Sci* 1987, 33, 1533.
11. Scott, G. *Mechanisms of Polymer Degradation and Stabilisation*; Elsevier Applied Science: London and New York, 1990.
12. Grassie, N.; Scott, G. *Polymer Degradation and Stabilisation*; Cambridge University Press: New York, 1988.
13. Kryszewski, M. *Polymer Blends. Processing, Morphology and Properties*; Plenum Press: New York, 1980.
14. Wunderlich, B. *Macromolecular Physics*, Vol. 1; Academic Press: New York, 1973; p 388.
15. Hawkins, W. *Polymer Degradation and Stabilization*; Springer-Verlag: Berlin, 1984.
16. Albertsson, A.-C.; Andersson, S. O.; Karlsson, S. *Polym Degrad Stabil* 1987, 18, 73.
17. Amin, M.-B.; Hamid, S. H.; Rahman, R. *J Appl Polym Sci* 1995, 56, 279.
18. Hamid, S. H.; Amin, M. B. *J Appl Polym Sci* 1995, 55, 1385.
19. Albertsson, A.-C.; Karlsson, S. *Prog Polym Sci* 1990, 15, 177.
20. McCrum, N. G.; Read, B. E.; Williams, G. *Anelastic and Dielectric Effects in Polymeric Solids*; Dover Publications: New York, 1991.
21. Boyd, R. H. *Polymer* 1985, 26, 323.
22. Popli, R.; Glotin, M.; Mandelkern, L. *J Appl Polym Sci Polym Phys* 1987, 22, 407.
23. Ribes-Greus, A.; Díaz-Calleja, R. *J Appl Polym Sci* 1987, 34, 2819.
24. Contat Rodrigo, L. Ph.D. thesis, Valencia, 2000.
25. Contat-Rodrigo, L.; Ribes-Greus, A.; Díaz-Calleja, R. *J Appl Polym Sci* 2001, 82, 2174.
26. Charlesworth, J. M. *J Mater Sci* 1993, 28, 399.